

Kinetic analysis of the soldering reaction between eutectic SnPb alloy and Cu accompanied by ripening

H. K. Kim and K. N. Tu

Department of Materials Science and Engineering, University of California at Los Angeles, Los Angeles, California 90095-1595

(Received 18 September 1995; revised manuscript received 20 February 1996)

The wetting reaction of molten eutectic SnPb on Cu leads to Cu-Sn intermetallic compound formation, but not compounds of Cu-Pb since they do not exist. Cu-Sn compounds do not form layered structures between the solder and Cu, rather the Cu_6Sn_5 phase has grown as scalloplike grains into the molten solder. The scalloplike grains grow larger but fewer with time, indicating that a ripening reaction has occurred among them. However, the ripening is not a constant volume process since it is accompanied by the soldering reaction. Between the scallop grains, there are molten solder channels extending nearly all the way to the Cu interface. In aging, these channels serve as fast diffusion and dissolution paths of Cu in the solder to feed the reaction. A kinetic analysis of the soldering reaction accompanied by the ripening reaction is given. In the analysis, the growth of the scalloplike grains is supplied by two fluxes: the flux of interfacial reaction and the flux of ripening. The latter was formulated by the Gibbs-Thomson equation. The former was obtained by measuring the rate of consumption of Cu in the reaction. The measurement was carried out by determining the change of the total volume of scalloplike grains (and in turn, the Cu content in the grains) as a function of time and temperature. A reasonable agreement has been obtained between the calculated scallop-grain growth based on kinetic analysis and the experimentally measured values. A discussion of the Cu consumption rate is given, since it is important for applications in electronic packaging technology. [S0163-1829(96)00823-5]

I. INTRODUCTION

Owing to the advance in very large-scale integration technology, there is a critical need for a large number of input/output (I/O) connections in packaging the Si chip.¹⁻³ To achieve a high density of I/O connections, the trend is to move from peripheral wire bonds to area array solder bumps. In optoelectronic technology, solder bumps are being adopted for automatic alignment in joining waveguides and laser chips.^{4,5} Therefore there is a renewed interest in solder technology for small interconnections, and a concern about their performance and reliability.

At present, solder technology is based on SnPb alloys. The Pb-bearing solder has nevertheless caused environmental concerns, due to toxic effects on underground water by land filling of discarded electronic products. There are four anti-Pb bills in Congress, and one was submitted by the Environmental Protection Agency to remove Pb from electronic packaging applications.⁶ In anticipation, the electronic industry is conducting a concerted effort in searching for Pb-free solders. Consequently, the science of soldering reactions, with and without Pb, has received much attention lately.

The essence of the soldering reaction is the formation of Cu-Sn intermetallic compounds. This is because there are no Cu-Pb compounds,⁷ so the only compound formation is that of Cu-Sn when we solder Cu electrodes. We might then ask what is the purpose of adding Pb to the solder, and what is its effect on the soldering reaction? These questions have led us to perform a systematic study of the interfacial reaction between molten eutectic SnPb solder and solid Cu substrate, and to understand the kinetics of Cu-Sn compound formation. In our preliminary study,⁸ we have observed a very unusual morphology of the growth of Cu-Sn compound

grains in soldering reactions. It is not a layered growth which is typical for interfacial compound formation. Rather the Cu-Sn compound growth has a scallop-type appearance, and is accompanied by a ripening reaction among the scallops. No kinetic analysis of such nonlayered compound growth has been given. Besides the eutectic SnPb/Cu reaction, we observed similar scallop-type morphology in reaction between eutectic SnBi and Cu, and also between eutectic SnAg and Cu, as shown in Fig. 1. It is rather general.

In this paper, we present a kinetic model to describe the interfacial reaction forming scallop grains accompanied by ripening. We shall first briefly review the growth morphology.

II. SCALLOP-TYPE GRAIN GROWTH AT SOLDER INTERFACE

Experimentally, the eutectic SnPb/Cu sample was prepared by melting the eutectic (63Sn37Pb, wt %) SnPb alloy on a Cu plate in mildly activated rosin flux (RMA). The rosin flux was used to improve the wettability of molten solder by removing the surface oxide on the Cu plate. The electropolished Cu (99.95% purity) plate was fully immersed in the heated flux at a given temperature with ± 3 °C control, and then a small (~ 2.0 mg) solder ball was placed on the plate. The solder ball melted and spread out to wet the metal surface, forming a cap with a stable wetting angle of 11° at 200 °C. Then it was solidified by cooling after a given reflow time. To study the intermetallic compound formation at the solder joints, two kinds of the eutectic SnPb/Cu samples were prepared: cross-sectional samples and top-polished samples. We use a selective Pb etching to remove the solder in order to reveal the morphology of the interfacial Cu-Sn compounds.

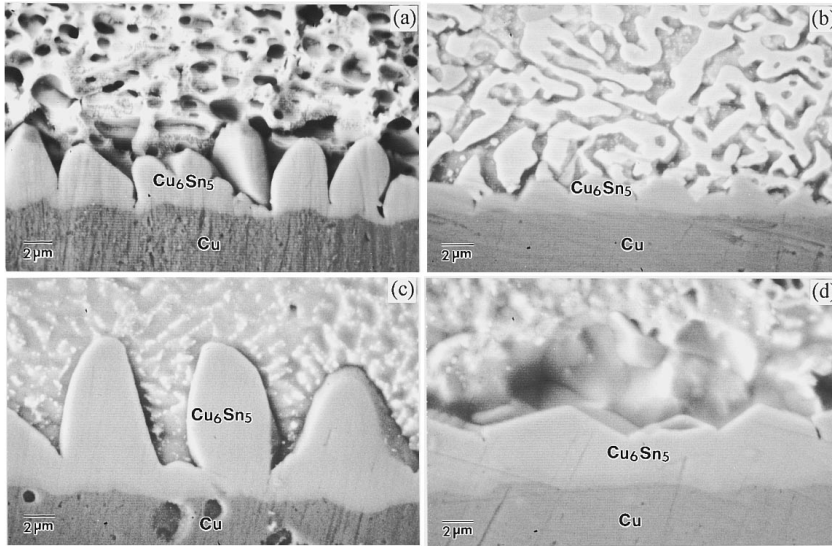


FIG. 1. Scallop-type morphology of Cu-Sn intermetallic compounds at the interface of solder/Cu. (a) Eutectic SnPb/Cu at 200 °C for 10 min. (b) Eutectic SnBi/Cu at 160 °C for 5 min. (c) Eutectic SnAg/Cu at 240 °C for 5 min. (d) Pure Sn/Cu at 250 °C for 5 min.

At the solder interface, two Cu-Sn compounds are formed: a scalloplike Cu_6Sn_5 phase and a thin layered Cu_3Sn phase. The Cu_6Sn_5 phase grew as scalloplike grains into the molten solder, and resulted in a very rough interfacial morphology between the compound and the solder. Three-dimensional morphology of the scalloplike grain has been presented to report the nature of the ripening reaction.⁸ As shown in Figs. 2(a) and 2(b), the scalloplike grains grow larger but fewer with time, indicating that a ripening reaction has occurred among them. The grain growth of Cu_6Sn_5 has an exponent of the usual bulk value of one-third.⁹ This shows that the Cu_6Sn_5 grains dispersed at the interface grow by a ripening process controlled by volume diffusion in the molten solder.

Between the Cu_6Sn_5 and Cu, a thin layer of the Cu_3Sn compound grows. However, the thickness of the layer is much smaller than the size of the scalloplike Cu_6Sn_5 grain. The thickness of the Cu_3Sn layer are 0.29 and 0.57 μm after 10- and 40-min reflows at 200 °C, as compared to sizes of 5.6 and 10.3 μm , respectively, of Cu_6Sn_5 . Between the Cu_6Sn_5 grains, there are molten solder channels extending all the way to the $\text{Cu}_3\text{Sn}/\text{Cu}$ interface. Since the Cu_3Sn compound layer is so thin, these channels serve as fast diffusion and dissolution paths of Cu in the solder to feed the interfacial reaction. Figure 2(c) shows that the ripening is not a constant volume process, since it is accompanied by an interfacial reaction between the solder and Cu. The nonconservative ripening growth is associated with the Cu supply through the channels. However, the ripening affects the rate of interfacial reaction. The reduction of the channel area by ripening growth might control the consumption rate of Cu during the reflow; it decreases with the time of reflow.

We propose a kinetic model for the grain growth of Cu_6Sn_5 . In the model, we describe grain growth by the coupling of two distinct processes: the ripening growth controlled by volume diffusion and the interfacial reaction growth.

III. KINETIC ANALYSIS

A. Ripening flux

In the analysis, the growth of the scalloplike grains is supplied by two fluxes of Cu atoms: the flux of interfacial

reaction and the flux of ripening. To consider the flux of Cu atoms due to the ripening reaction between scalloplike Cu_6Sn_5 grains, it is assumed that the grain is a hemisphere of radius r . Due to the Gibbs-Thomson effect,⁹⁻¹² the concentrations of Cu in the molten solder at the surface of the grain, C_r , will be

$$C_r = C_0 \exp\left(\frac{2\gamma\Omega}{rRT}\right) \quad (1)$$

and

$$C_r \cong C_0 \left[1 + \frac{2\gamma\Omega}{rRT} \right] \quad \text{if } \frac{2\gamma\Omega}{rRT} \ll 1, \quad (2)$$

where C_0 is equilibrium concentration of Cu in the solder, γ is interfacial energy per unit area between Cu_6Sn_5 and molten solder, Ω is the molar volume of Cu_6Sn_5 , R is a gas constant, and T is the temperature. Due to the curvature difference, the concentration gradient of Cu is set up in the molten solder between grains with different radius. That causes the ripening flux of Cu atoms going from the small grain to the larger grain, which permits the large grains to grow while the small ones shrink and disappear.

In the present case, the Cu_6Sn_5 grains are close together, and the mean separation $\bar{\delta}$ between grains is smaller than the mean grain radius \bar{r} . Therefore, the diffusion flux fields of adjacent grains will overlap, and the growth rate of grains will be dependent upon the grain-to-grain separation distance.¹³

In order to obtain the ripening flux of Cu atoms between closer grains, we consider the i th Cu_6Sn_5 grain and its nearest neighbors. Since the diffusion fields of Cu atoms between adjacent grains overlap each other, the tendency for dissolution or growth is determined mainly by the surrounding grains. For simplicity, we consider the ripening between the i th Cu_6Sn_5 grain and one neighboring grain with mean curvature. Figure 3 shows the concentration variation between the i th Cu_6Sn_5 grain and the mean grain. Although the Cu_6Sn_5 grains grow in spherical symmetry, the grains are dispersed only at the interface of solder and Cu in two dimensions. Therefore, we assumed a linear geometry of the

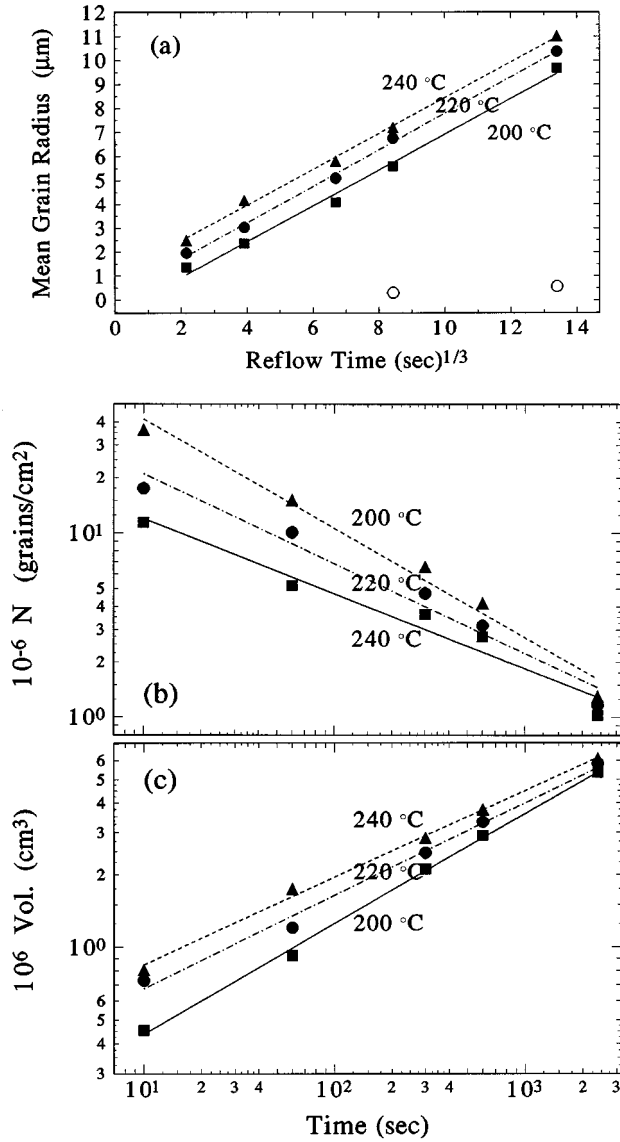


FIG. 2. For the Cu_6Sn_5 compound grains at the interface of eutectic SnPb/Cu . (a) The mean grain radius vs (reaction time) $^{1/3}$ (the thickness of the Cu_3Sn layer is indicated by “○” after 10 and 40 min at 200 °C). (b) The number of grains per unit interfacial area vs reaction time. (c) Total volume of grains vs reaction time.

system to determine the ripening flux. Later, in the Appendix, we present the solution for ripening flux in spherical symmetry.

Using the quasi-steady-state approximation, the flux of Cu atoms due to the concentration gradient is

$$J = -D \frac{dC}{dx} = -D \frac{\bar{C} - C_i}{\bar{\delta}}, \quad (3)$$

where D is the diffusivity of Cu in the molten solder.

From Eq. (2),

$$\bar{C} - C_i = \frac{2\gamma\Omega C_0}{RT} \left[\frac{1}{\bar{r}} - \frac{1}{r_i} \right], \quad (4)$$

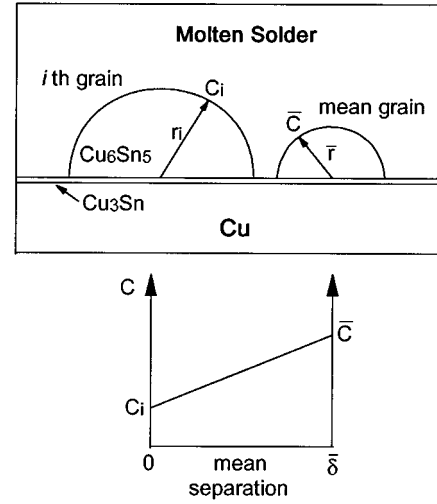


FIG. 3. Schematic representation of the concentration variation between the i th grain and a mean grain of different radius.

$$J = -D \frac{\bar{C} - C_i}{\bar{\delta}} = -\frac{2\gamma\Omega DC_0}{RT} \frac{1}{\bar{\delta}} \left[\frac{1}{\bar{r}} - \frac{1}{r_i} \right]. \quad (5)$$

Equation (5) can be simplified if we relate the mean separation $\bar{\delta}$ to the mean grain size \bar{r} . Since the mean separation between grains is smaller than the mean grain radius, $\bar{\delta} < \bar{r}$, we take $\bar{\delta} = L\bar{r}$, where $0 < L < 1$,

$$J = -\frac{2\gamma\Omega DC_0}{LRT} \frac{1}{\bar{r}} \left[\frac{1}{\bar{r}} - \frac{1}{r_i} \right]. \quad (6)$$

Furthermore, since the flux J has a maximum at r_i^{\max} in the distribution of grains, we use r_i^{\max} for \bar{r} and assume the largest size $r_i^{\max} = \frac{3}{2}\bar{r}$ for a typical value¹²

$$J^{\max} = -\frac{2\gamma\Omega DC_0}{LRT} \frac{1}{\bar{r}} \left[\frac{1}{\bar{r}} - \frac{2}{3\bar{r}} \right] = -\frac{2\gamma\Omega DC_0}{3LRT} \frac{1}{\bar{r}^2}. \quad (7)$$

Then the flux of ripening between the i th Cu_6Sn_5 grain and the mean grain with radius \bar{r} per unit area and unit time is

$$J^R = \frac{2\gamma\Omega DC_0}{3LRT} \frac{1}{\bar{r}^2}. \quad (8)$$

B. Interfacial reaction flux

The ripening reaction between the Cu_6Sn_5 grains is not a constant volume process because it is accompanied by the interfacial reaction between the solder alloy and Cu. Between the Cu_6Sn_5 grains, there are molten solder channels extending nearly all the way to the solder/Cu interface. While a thin layer of Cu_3Sn compound forms between the solder and Cu, the thickness of the layer is only $0.29 \mu\text{m}$ after 10 min at 200 °C. Therefore, Cu atoms can diffuse through the Cu_3Sn and dissolve quickly into the molten solder through the channels between the Cu_6Sn_5 grain rather than through the Cu_6Sn_5 grains themselves. During the reaction, these channels serve as fast diffusion and dissolution paths of Cu in molten solder. This kind of fast diffusion path has been reported in the literature.¹⁴ However, because the

Cu_6Sn_5 is not a layered compound, we cannot use a layered model to determine the flux of the interfacial reaction.

In order to determine the interfacial reaction flux of Cu atoms, we assume that the total loss of Cu from the substrate is equal to the total amount of Cu dissolved through channels,

$$\rho A \Delta h = \frac{m}{N_A} \int J^{IT} dt, \quad (9)$$

where ρ is the density of Cu, A is the total area of the solder/Cu interface, Δh is the consumed thickness of Cu, $A \Delta h$ is the consumed volume of Cu, m is the atomic mass of Cu, N_A is Avogadro's number, and J^{IT} is the total flux of Cu atoms through channels. Then the total interfacial reaction flux is

$$J^{IT} = \rho \frac{N_A}{m} A \nu, \quad (10)$$

where $\nu = dh/dt$ is the consumption rate of Cu in the reaction. If we assume that J^{IT} is uniformly distributed over all the surfaces of hemispherical Cu_6Sn_5 grains, the atomic flux of Cu diffusing into a surface element of grain of mean radius \bar{r} is

$$J^I = \frac{J^{IT}}{2\pi\bar{r}^2 N_p} = \frac{\rho N_A A \nu(t)}{2\pi m N_p(t)} \frac{1}{\bar{r}^2}, \quad (11)$$

where $2\pi\bar{r}^2$ is the surface area of a hemispherical Cu_6Sn_5 grain, and $N_p(t)$ is the total number of grains at interface. This shows that we can calculate J^I by measuring $N_p(t)$ and $\nu(t)$ in the reaction. We note that both $N_p(t)$ and $\nu(t)$ are time dependent.

C. Total flux

The growth of scalloplike Cu_6Sn_5 grains occurs through combined kinetic processes of ripening and interfacial reaction. Using Gauss' theorem, for a Cu_6Sn_5 grain of radius r , the total number of Cu atoms/s diffusing into a hemispherical Cu_6Sn_5 grain is

$$\begin{aligned} (\nabla \cdot \mathbf{J})V &= \int_A (\mathbf{J} \cdot \mathbf{n}) dA, \\ (\nabla \cdot J^I)V &= \{\nabla \cdot (J^R + J^I)\}V \\ &= \int_A \{(J^R|_{\bar{r}=r} + J^I|_{\bar{r}=r})n\} dA \\ &= -2\pi r^2 \left\{ \frac{2\gamma\Omega DC_0}{3LRT} \frac{1}{r^2} + \frac{\rho N_A A \nu(t)}{2\pi m N_p(t)} \frac{1}{r^2} \right\}. \end{aligned} \quad (12)$$

If the number of moles of Cu_6Sn_5 in a hemispherical grain with radius of r is Q , then the number of Cu atoms, Q^{Cu} , is

$$Q^{\text{Cu}} = 6N_A Q = 6N_A \frac{V}{\Omega}, \quad (13)$$

and

$$\frac{dQ^{\text{Cu}}}{dt} = 6N_A \frac{1}{\Omega} \frac{dV}{dt} = 6N_A \frac{2\pi r^2}{\Omega} \frac{dr}{dt}, \quad (14)$$

where $V = \frac{2}{3}\pi r^3$ is the volume of a hemispherical grain with a radius of r .

From the continuity equation, $-(\nabla \cdot J^I)V = dQ^{\text{Cu}}/dt$, then the growth rate of the Cu_6Sn_5 grain with radius of r is

$$\frac{dr}{dt} = \frac{\Omega}{6N_A} \left\{ \frac{2\gamma\Omega DC_0}{3LRT} + \frac{\rho N_A A \nu(t)}{2\pi m N_p(t)} \right\} \frac{1}{r^2}, \quad (15)$$

$$\int r^2 dr = \frac{\Omega}{6N_A} \int \left(\frac{2\gamma\Omega DC_0}{3LRT} + \frac{\rho N_A A \nu(t)}{2\pi m N_p(t)} \right) dt. \quad (16)$$

Thus the growth equation is

$$r^3 = \int \left(\frac{\gamma\Omega^2 DC_0}{3N_A LRT} + \frac{\rho A \Omega \nu(t)}{4\pi m N_p(t)} \right) dt. \quad (17)$$

The growth of the scalloplike Cu_6Sn_5 grains in the soldering reaction of eutectic SnPb on Cu consists of fluxes of interfacial and ripening reactions. The first term on the right-hand side of Eq. (17) is the ripening term, and the second term is the interfacial reaction term.

IV. RESULTS AND DISCUSSION

A. Morphology of interfacial compound formation

Solid-state interdiffusion typically leads to the formation of layered structures. This is generally true in reacting a bilayer of metals or a metal on semiconductors.^{15,16} The intermetallic compounds between the reactants become diffusion barriers, resulting in a diffusion-controlled layer growth. In certain cases, interfacial-controlled layer growth can take place. Kinetic analysis of these growths has been given,^{17,18} but not the ripening of scallop-type growth as presented here.

It is interesting to ask why this kind of growth occurs. The solder reaction is a liquid-solid reaction, where the solubility and diffusivity in the liquid state are usually large. The factors may enhance the ripening rate. It is a ternary system in which the Pb does not react with Cu to form compounds. While Pb does not react with Cu, it controls the melting temperature, limits the Cu-Sn reaction, retards the growth of Sn whiskers, and lends ductility to the joints.¹⁹ Also, Pb has a lower surface tension than Sn.²⁰ Therefore, Pb lowers the surface tension in Sn-Pb alloys, and it improves the wettability of solders. However, due to the selective reaction of Cu-Sn, the Pb must be expelled into the molten solder when Cu reacts with Sn. The Pb keeps the channel molten. In the case of eutectic SnBi/Cu and eutectic SnAg/Cu, Cu also does not react with Bi and Ag.⁷ In both cases, therefore, we observed similar scallop-type intermetallic compounds at the interface. In comparison, we found, as shown in Fig. 1(d), that when pure molten Sn reacts with Cu, a layered Cu-Sn compound tends to form, rather than the scallops.

B. Comparison of model with experimental results

To evaluate the growth equation given by Eq. (17), we take the experimental data from our measurement: $A = 9.16 \times 10^{-3} \text{ cm}^2$, $\nu = 2.736 \times 10^{-6} t^{-0.542} \text{ cm/s}$, and $N_p = 1.484 \times 10^6 t^{-0.592}$ grains at 200 °C.²¹ Material constants

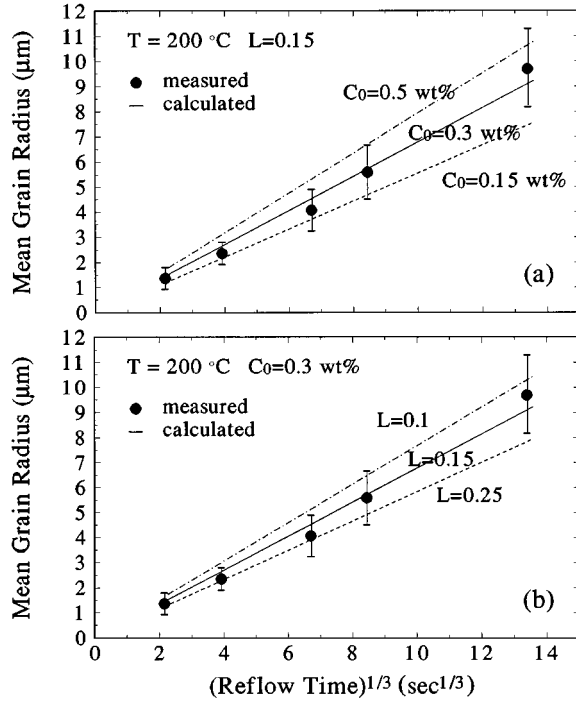


FIG. 4. The mean grain radius vs. (time)^{1/3} for eutectic SnPb/Cu (a) for $L=0.15$, and (b) for $C_0=0.3$ wt % of Cu.

are given^{22,23} as $\Omega=117.87$ cm³/mole of Cu₆Sn₅, $\rho_{\text{Cu}}=8.96$ g/cm³, $\rho_{\text{Cu}_6\text{Sn}_5}=8.27$ g/cm³, and $\rho_{\text{SnPb}}=8.46$ g/cm³. The eutectic SnPb solder is molten at 200 °C, and in the liquid state the diffusion coefficient is not very sensitive to temperature, so we take $D=10^{-5}$ cm²/s.²⁴ Since there are no data available for $\gamma_{\text{Cu}_6\text{Sn}_5/\text{solder}}$, we take $\gamma_{\text{Cu}/\text{solder}}=9\times 10^{-6}$ J/cm² for the $\gamma_{\text{Cu}_6\text{Sn}_5/\text{solder}}$.²⁵ Also, there is an uncertainty in the solubility of Cu in molten solder and the separation constant L . Therefore, we use a range of their values in our evaluation: $C_0=0.15$ wt %–0.5 wt % of Cu atoms in solder, $L=0.1$ –0.25 for the separation constant.

In Fig. 4, the calculated value of the grain size using Eq. (17), and the measured value at 200 °C, are plotted to check the kinetic analysis combining the ripening and interfacial reactions. From the results, we see that $L=0.15$ and $C_0=0.3$ wt % are a pair of the better-fitted values to the experimental data for intermetallic compound growth at 200 °C. Although the experimental data have some deviation from the $t^{1/3}$ growth, the agreement seems reasonable. Using the set of better-fitted values, we calculated the two fluxes of the ripening and the interfacial reaction to see which term is dominant in the reaction. Figure 5 shows that the ripening flux is dominant, about one order of magnitude greater than the interfacial reaction flux.

Since the diffusion of Cu atoms through the Cu₃Sn phase can limit the dissolution of Cu, we have used the interdiffusion coefficient in Cu₃Sn phase, $\bar{D}\cong 7\times 10^{-11}$ cm²/s,^{26,27} to calculate the atomic flux of Cu. After 10 min at 200 °C, the atomic flux deduced from the \bar{D} value is about 2×10^{14} atoms/cm² s, and it has the same order as the interfacial reaction flux of the kinetic model shown in Fig. 5. This means that the Cu₃Sn is not a diffusion-barrier limiting soldering reaction.

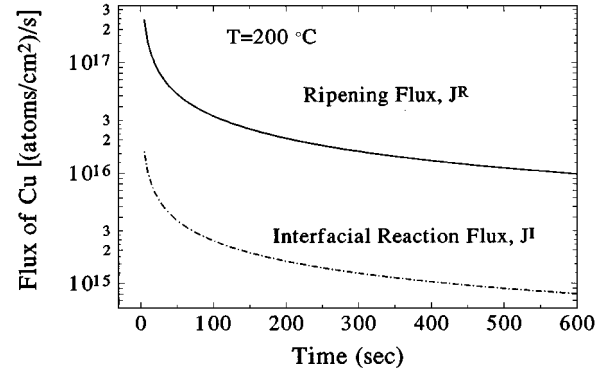


FIG. 5. The flux of Cu atoms in the reaction of eutectic SnPb/Cu at 200 °C for $L=0.15$ and $C_0=0.3$ wt % of Cu.

The solder reaction on the Cu sheet has an unlimited Cu source; the results might be different from the solder reaction on Cu thin-film metallization in electronic devices, where the Cu source is finite. Consequently, the ripening reaction will become a constant volume process. The reaction between the solder and the thin-film metallization needs to be studied.

C. Activation energy of Cu consumption

The flux of the interfacial reaction in the above analysis was obtained by measuring the rate of consumption of Cu in the reaction. The measurement was carried out by determining the change of the total volume of scalloplike grains, and in turn the Cu content in the grains, as a function of time and temperature.²¹ The Cu consumption rate is itself an important information for electronic packaging technology. The rate of Cu consumption during soldering must be under control, so that some unreacted Cu should be available for rework without dewetting.

Since the solubility of Cu in molten SnPb solder was determined from our analysis to be 0.3 wt % at 200 °C, we assume that the total loss of Cu from the Cu substrate is equal to the sum of Cu in the Cu-Sn compounds and in the liquid solder. Using cross-sectional and top-polished samples, we have measured the total volume of Cu-Sn intermetallic compounds. From the mass balance of Cu,²¹ we deduced the thickness of Cu consumed. The consumed thickness and the consumption rate are summarized in Table I. We note that it is difficult to measure the submicron thickness changes of the Cu directly, except to use tedious cross-sectional transmission electron microscopy. This is the reason why very little data for the consumption rate of Cu are available in the literature.

The time and temperature dependence of the Cu consumption reaction can be described by the kinetic equation

$$\Delta h = A \exp\left(\frac{-Q}{kT}\right) t^n, \quad (18)$$

where Δh is the consumed thickness of Cu, Q is the activation energy, k is the Boltzmann constant, T is the reaction temperature, t is the reaction time, and A and n are parameters. The values of n have been found to be 0.37, 0.34, and 0.32 for the reactions at 200, 220, and 240 °C, respectively.

The activation energy Q for the Cu consumption was determined using an Arrhenius plot based upon the equation

TABLE I. Copper consumption data during reflow with eutectic SnPb solder.

| time (s) | 200 °C | | 220 °C | | 240 °C | |
|----------|------------------------------|---|------------------------------|---|------------------------------|---|
| | Δh (μm) | $dh/dt \times 10^3$ ($\mu\text{m/s}$) | Δh (μm) | $dh/dt \times 10^3$ ($\mu\text{m/s}$) | Δh (μm) | $dh/dt \times 10^3$ ($\mu\text{m/s}$) |
| 10 | 0.26 | 7.85 | 0.35 | 9.75 | 0.42 | 12.04 |
| 60 | 0.48 | 2.97 | 0.62 | 3.41 | 0.73 | 3.84 |
| 300 | 0.90 | 1.24 | 1.08 | 1.33 | 1.23 | 1.38 |
| 600 | 1.21 | 0.85 | 1.38 | 0.89 | 1.56 | 0.89 |

$$\ln t_x = \frac{Q}{nkT} + \text{const}, \quad (19)$$

where t_x is the time required for Cu consumption of x - μm thickness at temperature T . As estimated from the slope in Fig. 6, the activation energy for the consumption of 0.5- and 1- μm thicknesses of Cu are equal to 0.29 and 0.19 eV, respectively, in the range of temperature between 200 and 240 °C. As a comparison, in the liquid Sn/Cu reaction, the activation energy for the diffusion of Cu into liquid Sn was determined by Ma and Swalin²⁸ to be 0.18 eV in the range of 240–480 °C.

V. SUMMARY

The kinetics of the wetting reaction of a molten eutectic SnPb alloy on Cu has been studied. We have observed the very unusual morphology of the growth of Cu-Sn compound grains at the interface of solder/Cu. The Cu_6Sn_5 grain growth has a scallop-type appearance, and is accompanied by ripening. A kinetic model is given to describe the growth of the scalloplike Cu_6Sn_5 grains by combining the interfacial reaction and the ripening. From the results of calculation, the model is better fitted to the experimental data when $L=0.15$ and $C_0=0.3$ wt % for compound growth at 200 °C.

The activation energy for Cu consumption in the soldering reaction was determined. The activation energies measured for the consumption of 0.5- and 1- μm thicknesses of Cu are equal to 0.29 and 0.19 eV, respectively, in the temperature range between 200 and 240 °C.

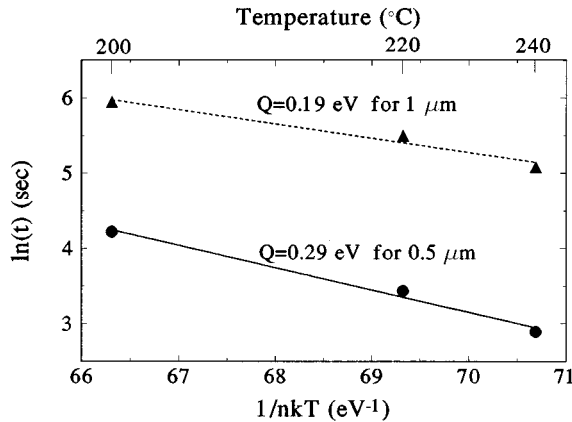


FIG. 6. Arrhenius plot of Cu consumption to determine activation energies.

ACKNOWLEDGMENTS

This research was supported by NSF Contract No. DMR-9320769 and SRC Contract No. 93-MJ-356. The authors wish to thank Dr. Ranjan J. Mathew and Dr. Luu Nguyen (National Semiconductor), Dr. Paul Totta (IBM East Fishkill Facility), Dr. Donald C. Abbott (Texas Instruments), and Professor A. J. Ardell (University of California at Los Angeles) for valuable discussions.

APPENDIX: RIPENING FLUX IN SPHERICAL COORDINATES

The hemispherical Cu_6Sn_5 grains are dispersed in two dimensions at the interface only; however, they grow in spherical symmetry. Therefore, we considered a dispersed system in spherical coordinates, where the i th grain centered at origin and the nearest neighbors with mean curvature dispersed only at the interface. Figure 7 shows the geometry of the dispersed system.

Let us consider the volume diffusion of Cu atoms in spherical coordinates (r, θ, ϕ) , where $0 \leq \theta \leq 2\pi$ and $0 \leq \phi \leq \pi/2$. Since the concentration of Cu is independent of θ , Fick's second law in spherical coordinates at a steady state is

$$\frac{\partial}{\partial r} \left(r^2 \frac{\partial C}{\partial r} \right) + \frac{1}{\sin \phi} \frac{\partial}{\partial \phi} \left(\sin \phi \frac{\partial C}{\partial \phi} \right) = 0, \quad (A1)$$

where r is the distance from the center of the i th grain, and $C(r, \phi)$ is the local concentration of Cu atoms. By the method of separating variables, we can solve Eq. (A1). Substituting a solution of the form $C(r, \phi) = G(r)H(\phi)$ into Eq. (A1), we obtain

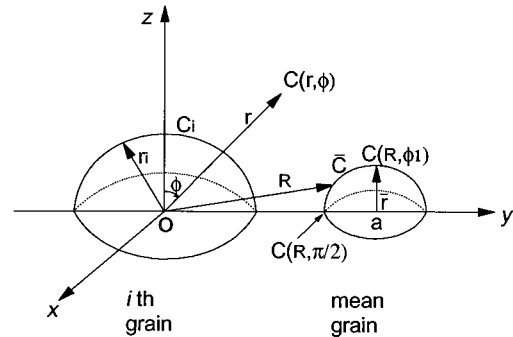


FIG. 7. The geometry of the dispersed system of a hemispherical i th grain and its nearest mean grain in spherical symmetry.

$$\frac{1}{G} \frac{d}{dr} \left(r^2 \frac{dG}{dr} \right) = k \quad (\text{A2})$$

and

$$\frac{1}{\sin \phi} \frac{d}{d\phi} \left(\sin \phi \frac{dH}{d\phi} \right) + kH = 0, \quad (\text{A3})$$

where k is a constant.

The solutions of the former equation are r^n and $1/r^{n+1}$, and the latter equation has solutions of the Legendre polynomials $P_n(\cos \phi)$, where n are integers. Thus we can write the concentration $C(r, \phi)$ as a linear combination of the Legendre polynomials,

$$C(r, \phi) = \sum_{n=0}^{\infty} A_n r^n P_n(\cos \phi) + \sum_{n=0}^{\infty} B_n \frac{P_n(\cos \phi)}{r^{n+1}}, \quad (\text{A4})$$

where n are integers, and A_n and B_n are constants. No θ dependence appears because of the axial symmetry of the problem.

Now we use boundary conditions to determine the unknown A_n and B_n of the series solution. At infinity, the concentration will be the equilibrium value C_0 , and

$$\lim_{r \rightarrow \infty} C(r, \phi) = C_0 \quad \text{when } r \rightarrow \infty, \quad (\text{A5})$$

where C_0 is the equilibrium concentration of Cu in the solder. From this infinity condition and Eq. (A4), we have

$$A_0 = C_0 \quad \text{and} \quad A_n = 0 \quad \text{for } n \geq 1,$$

then Eq. (A4) will be

$$C(r, \phi) = C_0 + \sum_{n=0}^{\infty} B_n \frac{P_n(\cos \phi)}{r^{n+1}}. \quad (\text{A6})$$

In this analysis, we consider the i th and its nearest-neighbor grains only. Since the local concentration of Cu, $C(r, \phi)$, is set up by the contribution of the i th grain and its nearest-neighbor grains, we assume that

$$C(r, \phi) = C_I(r, \phi) + C_{II}(r, \phi), \quad (\text{A7})$$

where $C_I(r, \phi)$ is the concentration due to the i th grain, and $C_{II}(r, \phi)$ is that due to the mean grain of nearest neighbors.

Case I: We consider the i th grain only for $0 \leq \phi \leq \pi/2$,

$$C_I(R_i, \phi) = C_i \quad \text{when } r = r_i, \quad (\text{A8})$$

where r_i is the radius of the i th grain centered at the origin, and C_i is the concentration of Cu induced by the Gibbs-Thomson effect at the surface of the i th grain. In this region, the concentration is dependent only on the i th grain, and it will be

$$C_I(r, \phi) = C_0 + \sum_{n=0}^{\infty} B_{In} \frac{P_n(\cos \phi)}{r^{n+1}}, \quad (\text{A9})$$

and from condition (A8),

$$C_I(r_i, \phi) = C_0 + \sum_{n=0}^{\infty} B_{In} \frac{P_n(\cos \phi)}{r_i^{n+1}} = C_i, \quad (\text{A10})$$

$$\sum_{n=0}^{\infty} B_{In} \frac{P_n(\cos \phi)}{r_i^{n+1}} = C_i - C_0. \quad (\text{A11})$$

Since Eq. (A11) is the generalized Fourier series of $C_i - C_0$ in terms of Legendre polynomials, we have

$$B_{In} = \frac{2n+1}{2} r_i^{n+1} \int_0^{\pi/2} (C_i - C_0) P_n(\cos \phi) \sin \phi \, d\phi. \quad (\text{A12})$$

Case II: We consider the mean grain only at the nearest-neighbor distance. Since the grains are dispersed at the interface only as shown in Fig. 7, we divide the boundary into two regions: $0 \leq \phi < \phi_1$ for the region of no neighbors, and $\phi_1 \leq \phi \leq \pi/2$ for the region having neighbors.

For $\phi_1 \leq \phi \leq \pi/2$, and $\phi_1 = \sin^{-1}(a/\sqrt{a^2 + \bar{r}^2})$,

$$C_{II}(R, \phi) = \bar{C} \quad \text{when } r = R, \quad (\text{A13})$$

where R is the distance from the origin to the surface of a mean grain, $R = a \sin \phi \pm \sqrt{a^2 \sin^2 \phi - (a^2 - \bar{r}^2)}$, a is the distance between the origin and the center of mean grain with a radius of \bar{r} , and \bar{C} is the concentration of Cu induced by the Gibbs-Thomson effect at the surface of the mean grain. In this region, the concentration of Cu due to a nearest mean grain, for $0 \leq \phi \leq \pi/2$, is

$$C_{II}(r, \phi) = C_0 + \sum_{n=0}^{\infty} B_{II n} \frac{P_n(\cos \phi)}{r^{n+1}}. \quad (\text{A14})$$

For Eq. (A14) to satisfy condition (A13), we must have

$$C_{II}(R, \phi) = C_0 + \sum_{n=0}^{\infty} B_{II n} \frac{P_n(\cos \phi)}{R^{n+1}} = \bar{C}, \quad (\text{A15})$$

$$\sum_{n=0}^{\infty} B_{II n} \frac{P_n(\cos \phi)}{R^{n+1}} = \bar{C} - C_0. \quad (\text{A16})$$

Then we have

$$B_{II n} = \frac{2n+1}{2} R^{n+1} \int_{\phi_1}^{\pi/2} (\bar{C} - C_0) P_n(\cos \phi) \sin \phi \, d\phi. \quad (\text{A17})$$

Case III: We consider the i th grain and its nearest neighbor together. By the superposition of two concentration terms of $C_I(r, \phi)$ and $C_{II}(r, \phi)$, we can derive the equation for the Cu concentration in the system. Since C_0 is the equilibrium concentration of Cu in the molten solder, using Eqs. (A7), (A12), and (A17) we have the solution

$$C(r, \phi) = C_0 + \sum_{n=0}^{\infty} (B_{In} + B_{II n}) \frac{P_n(\cos \phi)}{r^{n+1}}, \quad (\text{A18})$$

with coefficients

$$B_{In} = \frac{2n+1}{2} r_i^{n+1} \int_0^{\pi/2} (C_i - C_0) P_n(\cos \phi) \sin \phi \, d\phi,$$

$$B_{II n} = \frac{2n+1}{2} R^{n+1} \int_{\phi_1}^{\pi/2} (\bar{C} - C_0) P_n(\cos \phi) \sin \phi \, d\phi.$$

This is the concentration equation of Cu in the molten solder at a position of (r, ϕ) between the i th grain and nearest mean grain.

In a diffusion problem, the flux of atoms is given by

$$J = -D \frac{dC}{dr}, \quad (\text{A19})$$

where D is the diffusion coefficient of atoms. At a fixed value of r_i , using Eq. (A18), the flux equation of ripening between the i th grain and the mean grain is

$$J^R = -D \left. \frac{\partial C}{\partial r} \right|_{r_i} = D \sum_{n=0}^{\infty} \left\{ (B_{In} + B_{In}) \frac{(n+1)P_n(\cos\phi)}{r_i^{n+2}} \right\}. \quad (\text{A20})$$

If we use $r_i^{\max} = \frac{3}{2}\bar{r}$,

$$J^R = D \sum_{n=0}^{\infty} \left\{ (B_{In} + B_{In}) \frac{(n+1)P_n(\cos\phi)}{\left(\frac{3}{2}\right)^{n+2}\bar{r}^{n+2}} \right\}. \quad (\text{A21})$$

This is the flux equation for ripening of the i th grain in spherical coordinates.

Since $|P_n(\cos\phi)| \leq 1$ and $P_0(\cos\phi) = 1$, we consider Eq. (A21) for $n=0$, and then

$$J^R \propto \frac{1}{\bar{r}^2} \quad \text{for } n=0. \quad (\text{A22})$$

Therefore, we have reduced Eq. (A21) to Eq. (8), having the same $(1/\bar{r}^2)$ dependence, and this indicates that our linear assumption in the ripening flux is well matched to the spherical model for $n=0$.

-
- ¹ *Semiconductor Technology Workshop Working Group Reports Semiconductor Industry Association* (Semiconductor Research Cooperation, Research Triangle Park, NC, 1992).
- ² R. R. Tummala and E. J. Rymaszewski, *Microelectronics Packaging Handbook* (Van Nostrand Reinhold, New York, 1989).
- ³ D. Seraphim, R. Lasky, and C. Y. Li, *Principles of Electronic Packaging* (McGraw-Hill, New York, 1989).
- ⁴ R. A. Boudreau, *J. Met.* **46**, 41 (1994).
- ⁵ Y. C. Lee and N. Basavanahally, *J. Met.* **46**, 46 (1994).
- ⁶ R. N. Wild (unpublished).
- ⁷ M. Hansen, *Constitution of Binary Alloys* (McGraw-Hill, New York, 1958), p. 610.
- ⁸ H. K. Kim, H. K. Liou, and K. N. Tu, *Appl. Phys. Lett.* **66**, 2337 (1995).
- ⁹ J. H. Yao, K. R. Elder, H. Guo, and M. Grant, *Phys. Rev. B* **47**, 14 110 (1993).
- ¹⁰ P. Haasen, *Physical Metallurgy*, 2nd ed. (Cambridge University Press, Cambridge, 1986), p. 214.
- ¹¹ A. J. Ardell, *Phase Transformations '87* (Institute of Metals, London, 1988), p. 485.
- ¹² I. M. Lifshitz and V. V. Sloyozov, *J. Phys. Chem. Solids* **19**, 35 (1961).
- ¹³ S. Sarian and H. W. Weart, *J. Appl. Phys.* **37**, 1675 (1966).
- ¹⁴ F. Bartels, J. W. Morris, Jr., G. Dalke, and W. Gust, *J. Electron. Mater.* **23**, 787 (1994).
- ¹⁵ M. Natan, S. W. Duncan, and N. E. Byer, *J. Appl. Phys.* **55**, 1450 (1984).
- ¹⁶ S. H. Chen, L. R. Zheng, C. B. Carter, and J. W. Mayer, *J. Appl. Phys.* **57**, 258 (1985).
- ¹⁷ U. Goesele and K. N. Tu, *J. Appl. Phys.* **53**, 3252 (1982).
- ¹⁸ D. A. Porter and K. E. Easterling, *Phase Transformations in Metals and Alloys* (Van Nostrand Reinhold, New York, 1981).
- ¹⁹ K. N. Tu and R. D. Thompson, *Acta Metall.* **30**, 947 (1982).
- ²⁰ D. W. G. White, *Metall. Trans.* **2**, 3067 (1971).
- ²¹ H. K. Kim and K. N. Tu, *Appl. Phys. Lett.* **67**, 2002 (1995).
- ²² *CRC Handbook of Materials Science, Vol 1: General Properties*, edited by C. T. Lynch (CRC, Cleveland, 1974).
- ²³ J. D. Bernal, *Nature* **122**, 54 (1928).
- ²⁴ C.-K. Hu, H. B. Huntington, and G. R. Gruzalski, *Phys. Rev. B* **28**, 579 (1983).
- ²⁵ G. C. Smith and C. Lea, *Surf. Interface Anal.* **9**, 145 (1986).
- ²⁶ D. A. Unsworth and C. A. Mackay, *Trans. Inst. Metal Finish* **54**, 68 (1976).
- ²⁷ M. Onishi and H. Fujibuchi, *Trans. Jpn. Inst. Metal* **16**, 539 (1975).
- ²⁸ C. H. Ma and R. A. Swalin, *Acta Metall.* **8**, 388 (1960).